A new crystallographic method for detecting space topology

J.-Ph. Uzan[1,2]**, R. Lehoucq**[3]**, and J.-P. Luminet**[2]

[1] Département de Physique Théorique, Université de Genève, 24 quai E. Ansermet, 1211 Geneva, Switzerland (uzan@amorgos.unige.ch)

[2] Département d'Astrophysique Relativiste et de Cosmologie, Observatoire de Paris, CNRS–UPR 176, 92195 Meudon, France
(Jean-Pierre.Luminet@obspm.fr)

[3] CE-Saclay, DSM/DAPNIA/Service d'Astrophysique, 91191 Gif sur Yvette cedex, France (roller@discovery.saclay.cea.fr)

Abstract. Multi–connected universe models with space identification scales smaller than the size of the observable universe produce topological images of cosmic sources. We generalise to locally hyperbolic spaces the crystallographic method, aimed to detect the topology from three–dimensional catalogs of cosmological objects. Our new method is based on the construction of a *collecting–correlated–pair* technique which enhances the topological signature and can make it detectable. The main idea is that in multi–connected universes, equal distances occur more often than by chance. We present an idealised version of this method as well as numerical simulations, we discuss the statistical relevance of the expected signature and we show how the extraction of a topological signal may also lead to a precise determination of the cosmological parameters. A more realistic version of the method which takes account of uncertainties in the position and velocity data is then discussed. We apply our technique to presently available data, namely a quasar catalog, and discuss the significance of the result. We show how the improved crystallographic method both competes with the two–dimensional methods based on cosmic microwave background analyses, and suffers from the same drawback: the shortage of present observational data.

Key words: cosmology: theory – cosmology: large-scale structure of Universe

1. Introduction

Recently there have been many advances in the development of methods to detect or constrain the topology of the universe (i.e. of its spatial sections). Since the revival of cosmic topology (see Lachièze-Rey & Luminet (1995) and the proceedings of the workshop *Cosmology and topology* (1998) for the latest developments) many methods using either the cosmic microwave background (see e.g. Stevens et al. (1993), de Oliveira Costa et al. (1996), Cornish et al. (1998a; 1998b; 1998c), Levin et al. (1997; 1998) and Uzan (1998a; 1998b)), or discrete sources such as clusters, quasars, etc. (see e.g. Lehoucq et al. (1996) and Roukema & Edge (1997)) were investigated. The latter

Send offprint requests to: J.-Ph. Uzan

class of methods is based on the fact that an observer in a multi-connected universe is looking at a finite part of its universal covering space (Ellis 1971). We thus expect to see multiple images of any object (Lachièze-Rey & Luminet 1995). This property was first applied to specific objects to provide bounds on the size of the universe using our Galaxy (Sokolov 1971; Fagundes & Wichoski 1987), the Coma cluster (Gott 1980; Roukema 1996) and quasars (Roukema & Edge 1997). It was then applied statistically through the so–called crystallographic method (Lehoucq et al. 1996), the applicability of which was discussed by Fagundes & Gausmann (1997) in Euclidean manifolds and by Lehoucq et al. (1999) in hyperbolic and elliptic manifolds, see also Gomero et al. (1998), Fagundes & Gausmann (1998). The crystallographic method is a statistical one which was framed as to extract characteristic lengths associated with the topology of the universe, and thus which gets around the problem of recognizing objects at different ages and orientations (Lehoucq et al. 1996).

Today, multi-connected universes with locally Euclidean spatial sections are well constrained both by the absence of a cut-off in the angular power spectrum of the cosmic microwave background temperature anisotropies (Stevens et al. 1993), and by the crystallographic method (Lehoucq et al. 1996; Uzan et al. 1999) which puts a lower bound on the characteristic size, L say, of Euclidean space models to $L \geq 3000 \, h^{-1} \mathrm{Mpc}$ (with $h = H_0/100 \, \mathrm{km \, s^{-1} Mpc^{-1}}$, H_0 being the Hubble constant). But there is still no reliable constraint on a universe with locally hyperbolic spatial sections either from the cosmic microwave background methods (Inoue 1998; Bond et al. 1998) or from the clusters and quasars catalogs (Lehoucq et al. 1999). Thus, the quest for cosmic topology will probably be longer than expected.

The goal of this article is to improve the crystallographic method so as to make it suitable for the detection of topology in locally hyperbolic spaces. For that purpose, we first review the crystallographic method in Sect. 2, comment on its applicability and also on recent attempts at its improvement and generalisation. This leads us to propose a new method to detect the topology using a catalog of discrete sources (Sect. 3), aimed to enhance the topological signal by collecting all correlated pairs of images. We first apply the technique to simulated catalogs

(Sect. 4) in order to study its statistical relevance, then to a real catalog of more than $11,000$ quasars (Sect. 5). We discuss this result after having studied all the uncertainties in the implementation of the method and in real data.

2. Ups and downs of the crystallographic method

Assuming that the four–dimensional manifold $\mathcal{M}$ describing the universe is globally hyperbolic (Hawking & Ellis 1973), which is the case since we reduce our study to universes which can locally be described by a Friedmann-Lemaître spacetime, it can be split as $\mathcal{M} = R \times \Sigma$ where the spatial sections Σ are locally homogeneous and isotropic.

Now, if the universe is multi-connected, Σ can be written as

$$\Sigma \equiv X/\Gamma, \tag{1}$$

where X is either the Euclidean space (E^3), the spherical space (S^3) or the hyperbolic space (H^3), and Γ is the holonomy group, namely a finite discrete subgroup without fixed point of the full isometry group of X (Lachièze-Rey & Luminet 1995). The determination of the universal covering X will be given by the knowledge of the cosmological parameters such as the density parameter Ω_0 and the cosmological constant Λ, which will help us to determine the local geometry (since Einstein's equations are partial differential equations, there is locally no difference between a multi– and a simply–connected universe).

The three–dimensional manifold Σ can be conveniently described by its fundamental domain, which is a polyhedron with $2K$ faces identified by pairs through the elements g of the holonomy group Γ (Lachièze-Rey & Luminet 1995). A classification of these manifolds can be found in Lachièze-Rey & Luminet (1995) for Euclidean and elliptic manifolds, and by using the software *SnapPea* (http://www.northnet.org/weeks) for hyperbolic manifolds, see also Thurston (1997) and Wolf (1984).

The crystallographic method (Lehoucq et al. 1996) relies on a property of multi–connected universes according to which each topological image of a given object is linked to the other one by the holonomies of space which are indeed unknown as far as the topology is not determined. The only thing we know is that these holonomies are isometries. For instance in a 3–torus universe, to each holonomy g is associated a distance λ_g, equal to the length of the translation by which the fundamental domain is moved to produce the tessellation in the covering space. Assuming the fundamental domain contains N objects (e.g. galaxy clusters), if we calculate the mutual 3D–separations between every pair of topological images (inside the particle horizon), the distances λ_g will occur at least N times for each copy of the fundamental domain, and all other distances will be spread in a smooth way between zero and two times the horizon distance. In a pair separation histogram which plots the number of pairs versus their 3D–separations, the repetition scales λ_g should thus produce spikes. Simulations in locally Euclidean manifolds showed that the pairs between two topological images of the same object drastically emerge from ordinary pairs (Lehoucq et al. 1996) in the histogram.

As it was recently explained (Lehoucq et al. 1999), two kinds of pairs can create a spike, namely (we keep the notation and vocabulary introduced in Lehoucq et al. (1999))

1. *Type I pairs* of the form $\{g(x), g(y)\}$, since $\text{dist}[g(x), g(y)] = \text{dist}[x, y]$ for all points and all elements g of Γ.
2. *Type II pairs* of the form $\{x, g(x)\}$ if $\text{dist}[x, g(x)] = \text{dist}[y, g(y)]$ for at least some points and elements g of Γ.

It has been shown (Lehoucq et al. 1999; Gomero et al. 1998) that in hyperbolic manifolds, type II pairs will not exist since the holonomies are not Clifford translations (i.e. they are such that $\text{dist}[x, g(x)]$ depends on x).

Indeed, type I pairs are always present whatever the topology but their number is roughly equal to the number of copies of the fundamental polyhedron within the catalog's limit. This number is too small to create a spike in the pair separation histogram (Lehoucq et al. 1999) and depends on the cosmological parameters since a catalog of redshift depth z will contain all the objects located within the 2–sphere centered on the observer and of radius $\chi(z)$, the radial distance obtained by integration of the null geodesic equation up to a redshift z.

Two possible solutions were proposed to improve the crystallographic method in order to detect the topology and thus to extract the signature of type I pairs in catalogs.

1. Fagundes & Gaussmann (1998) developed a variant of the crystallographic method where they subtract the pair separation histogram for a simulated catalog in a simply-connected universe from the observed pair separation histogram (with the same number of objects and the same cosmological parameters). The result is "a plot with much oscillation on small scale, modulated by a long wavelength quasi-sinusoidal pattern". The statistical relevance of this signature still has to be investigated.
2. Gomero et al. (1998) proposed splitting the catalog into "smaller" catalogs and averaging the pair separation histograms built from each sub–catalog to reduce the statistical noise and extract a topological signal from what they call "the non-translational isometries". The feasability of this method has not yet been demonstrated.

We now develop a new method based on the property that whatever the topology, type I pairs will always exist. Indeed, as we have shown in Lehoucq et al. (Lehoucq et al. 1999), this does not lead to any observable spike in the pair separation histogram. We thus have to improve the crystallographic method to enhance the topological signature by "collecting" all these correlated pairs together. This can be achieved by defining what we call a *collecting correlated pair* method (hereafter CCP–method). Such an approach (described in detail in the next section) will not be able to determine the exact topology but will give a signature of the existence of at least one compact spatial dimension on sub–horizon scale, which is indeed a first step toward the determination of the topological scale of the universe. Once such a signature is obtained, many routes are possible to

determine the exact topology. We shall briefly refer to them in the final discussion.

3. How can we use a 3D-catalog to detect the topology of the universe?

3.1. Basic idea

As stressed in the former paragraph, type I pairs will always exist in multi–connected spaces as soon as one of the characteristic lengths of the fundamental domain, such as the injectivity radius r_{inj} (see, e.g., Fig. 10 in Luminet & Roukema (1999)), is smaller than the Hubble scale. Defining $g_i|_{1 \leq i \leq 2K}$ as the $2K$ generators of Γ and referring to x as the position of the image in the universal covering space X, we have:

1. $\forall x, y \in X, \forall g \in \Gamma$,

$$\text{dist}[g(x), g(y)] = \text{dist}[x, y]. \tag{2}$$

We will refer to these pairs as xy–pairs.

2. $\forall x \in X, \forall g_1, g_2 \in \Gamma$,

$$\text{dist}[g_1(x), g_1 \circ g_2(x)] = \text{dist}[x, g_2(x)]. \tag{3}$$

We will refer to these pairs as $xg(x)$-pairs.

Both the xy–pairs and the $xg(x)$-pairs are type I pairs.

To collect all these pairs and enhance the topological signal, we define the *CCP–index* of a catalog containing N objects as follows.

1. We compute all the 3D–distances $\text{dist}[x, y]$ for all pairs of points within the catalog's limit.
2. We order all these distances in a list $d_i|_{1 \leq i \leq P}$, where $P \equiv N(N-1)/2$ is the number of pairs, such that $d_{i+1} \geq d_i$.
3. We create a new list of increments defined by

$$\forall i \in [1...P-1], \quad \Delta_i \equiv d_{i+1} - d_i \tag{4}$$

(keeping all the equal distances, if any, in the list).

4. We then define the CCP-index $\mathcal{R}$ as

$$\mathcal{R} \equiv \frac{\mathcal{N}}{P-1}, \tag{5}$$

where $\mathcal{N} \equiv \text{card}(\{i, \Delta_i = 0\})$, so that $0 \leq \mathcal{R} \leq 1$.

With such a procedure, all type I pairs will contribute to $\mathcal{N}$. For instance, if a given distance appears 4 times in the list $d_i|_{1 \leq i \leq P}$, it will contribute to 3 counts in $\mathcal{N}$. Compared to the former crystallographic method, all the correlated pairs are gathered into a single spike, instead of being diluted into the noise of the histogram pair separation.

Indeed, in a more realistic situation, one has to take into account bins of finite width ϵ and replace $\mathcal{N}$ by

$$\mathcal{N}_\epsilon \equiv \text{card}(\{i, \Delta_i \in [0, \epsilon[\}) \tag{6}$$

in the computation of $\mathcal{R}$. The effect of such a binning will be discussed in Sect. 5. We now focus on the "idealised" version of the procedure and study the magnitude of the CCP–index in multi-connected models.

For that purpose, let us assume that the catalog is obtained from an initial set of A objects lying in the fundamental domain and that there are B copies of this domain within the catalog's limits ($B = 0$ if the whole observable universe up to the catalog's limit is included inside the fundamental domain). The total number of images is $N = A(B+1)$. Indeed B is not usually an integer but we assume it is, in order to *estimate* the amplitude of $\mathcal{R}$ and compare it with the result in a simply-connected model.

We now need to count the number of copies of a given pair.

1. Each xy–pair will be represented $B + 1$ times, so that the $A(A-1)/2$ pairs contribute to $BA(A-1)/2$ counts in $\mathcal{N}$.
2. For $xg(x)$-pairs, let $\nu_1(\Sigma, B)$ be the contribution to $\mathcal{N}$ when $A = 1$. For all $x \in \Sigma$, the total contribution of the $xg(x)$-pairs is then $A^2 \nu_1(\Sigma, B)$. $\nu_1(\Sigma, B)$ can be computed by considering a catalog generated from an initial set of $A = 1$ object and has the property that whatever the manifold Σ, $\nu_1(\Sigma, 0) = 0$ and $\nu_1(\Sigma, B)$ is an increasing function of B.
3. Summing these two type I pair contributions we obtain:

$$\mathcal{N}_{min} = A \left[(A-1)\frac{B}{2} + A\nu_1(\Sigma, B) \right]. \tag{7}$$

Indeed, if the holonomy group Γ contains Clifford translations allowing for type II pairs, or if there are "fake" pairs (i.e. such that $\text{dist}[x, y] = \text{dist}[u, v]$), $\mathcal{N}_{min}$ computed from (7) will give a lower bound for the true $\mathcal{N}$.

The normalised CCP–index (5) follows straightforwardly. $\mathcal{R}$ is a good index for extracting the topological signal since

1. when $B = 0$ (i.e. when the fundamental domain is greater than the catalog's spatial scale), $\mathcal{R} = 0$,
2. when the number of sources in the fundamental domain becomes important, it behaves as

$$\mathcal{R} \to \frac{B + 2\nu_1(\Sigma, B)}{(B+1)^2} \quad \text{as} \quad A \to \infty. \tag{8}$$

3.2. Application to a 2–dimensional flat manifold

As an illustrating example, we perform the computation in 2–dimensional flat manifolds, and more particularly in the case of the 2–torus T^2. Such a space contains Clifford translations, however we count only the contribution of type I pairs to $\mathcal{R}$. In that case, the only quantity which needs to be computed is $\nu_1(T^2, B)$.

Consider the 2–torus T^2 with its eight nearest neighbours ($B = 8$) [see Fig. 1 for the notation]. The pairs

- $(x, g_1(x))$ and $(x, g_4(x))$ appear 6 times,
- $(x, g_1 \circ g_2(x))$ and $(x, g_1 \circ g_4(x))$ appear 4 times,
- $(g_2 \circ g_3(x), g_1 \circ g_2(x))$ and $(g_2 \circ g_3(x), g_3 \circ g_4(x))$ appear 3 times,
- $(g_4(x), g_2 \circ g_3(x))$, $(g_4(x), g_1 \circ g_2(x))$, $(g_4(x), g_2 \circ g_3(x))$, $(g_3(x), g_1 \circ g_2(x))$ and $(g_3(x), g_1 \circ g_4(x))$ appear 2 times,

so that $\nu_1(T^2, 8) = 2 \times 5 + 2 \times 3 + 2 \times 2 + 4 \times 1 = 24$. This leads to $\mathcal{N} = 4A(7A - 1)$ whereas $P = 9A(9A - 1)/2$ so that

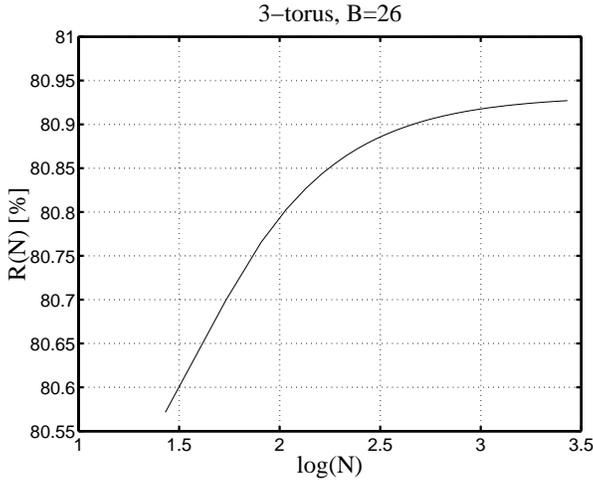$$\frac{24}{35} \leq \mathcal{R} \leq \frac{56}{81}, \quad \forall A \geq 1. \tag{9}$$

Fig. 1. Example of the 2–torus with $B = 8$. We have represented the different type I pairs that contribute to $\nu_1(T^2, 8)$.

Fig. 2. Example of the 3–torus with $B = 26$, convention for labelling the copies of the fundamental domain. The image of a point in the fundamental domain (at the center) is mapped into the cell e.g. 123 by $g_1 \circ g_2 \circ g_3$.

Fig. 3. Example of the 3–torus. The different families of pairs that contribute to $\nu_1(T^3, 26)$ as labelled in the text starting from the base point in 456.

Using the same technique one could compute the same quantities for various 2–dimensional topologies such as hyperbolic n–holes tori.

3.3. Application to 3–dimensional manifolds

In the case of 3–dimensional manifolds, the computation of $\nu_1(\Sigma, B)$ follows the same lines as in the previous section. We just give two examples.

- **3–torus with its 26 nearest neighbours**: We use the numerotation of Fig. 2 and the notation[1] $123 \equiv g_1 \circ g_2 \circ g_3(x)$, $0 \equiv x$ etc. We find that the pairs

  a: $(0, 1)$, $(0, 2)$ and $(0, 3)$ appear 18 times,
  b: $(0, 12)$, $(0, 15)$, $(0, 23)$, $(0, 35)$, $(0, 16)$ and $(0, 13)$ appear 12 times,
  c: $(0, 123)$, $(0, 234)$, $(0, 345)$ and $(0, 135)$ appear 8 times,
  d: $(1, 4)$, $(2, 5)$ and $(3, 6)$ appear 9 times,
  e: $(12, 45)$, $(15, 24)$, $(13, 46)$, $(34, 16)$, $(23, 56)$ and $(35, 26)$ appear 3 times,
  f: $(1, 45)$, $(1, 24)$, $(2, 45)$, $(2, 15)$ and 8 other pairs obtained by permutations appear 6 times,
  g: $(6, 123)$, $(6, 234)$, $(6, 345)$, $(6, 135)$, $(1, 245)$, $(1, 456)$, $(2, 456)$, $(2, 156)$, $(4, 156)$, $(4, 126)$, $(5, 246)$ and $(5, 126)$ appear 4 times,
  h: $(24, 156)$, $(12, 456)$, $(15, 246)$, $(45, 126)$, $(13, 246)$, $(13, 456)$, $(23, 456)$, $(23, 156)$, $(43, 156)$, $(43, 126)$, $(53, 246)$ and $(53, 126)$ appear twice,
  i: $(123, 456)$ appears once,

  so that $\nu_1(T^3, 26) = 3 \times 17 + 6 \times 11 + 4 \times 7 + 8 \times 3 + 12 \times 5 + 12 \times 3 + 12 \times 1 + 1 \times 0 = 282$. The eight families of pairs are represented on Fig. 3. In that example about 80% of the increments are in $\mathcal{N}$. Again, we recall that when $A = 1$, we only collect type I pairs.

- **Weeks manifold with its 18 nearest neighbours**: This manifold (Weeks 1985) is the smallest known compact hyperbolic manifold. Its description can be found by using the software *SnapPea* where it has the closed census m003(-3,1). Its volume, in units of the curvature radius, is 0.94272 and its fundamental polyhedron has 18 faces (see also Ap-

pendix A in Lehoucq et al. (1999)). It can then be shown after (some tedious computations) that

$$\nu_1(\text{Weeks}, 18) = 90, \tag{10}$$

which implies that $\mathcal{N} = 9A(11A - 1)$.

The CCP–index $\mathcal{R}$ is given as a function of ν_1, A (the number of sources in the fundamental domain) and B (the number of copies of the domain within the observable universe) by:

$$\mathcal{R} = \frac{A[(2\nu_1 - B)A - B]}{(B + 1)^2 A^2 - (B + 1)A - 2}. \tag{11}$$

In Figs. 4 and 5 we plot $\mathcal{R}$ as a function of the number of objects N for the two 3–dimensional examples given above, respectively $\{T^3, 26\}$ ($N = 27A$) and $\{\text{Weeks}, 18\}$ ($N = 19A$).

By comparison, when computing numerically the CCP–index in a simply-connected Friedmann-Lemaître model with the same number of objects and copies, one gets $\mathcal{R}(N) \simeq 0$ with some negligible fluctuations.

Thus, in this idealised method (which neglects the thickness of the bin ϵ), $\mathcal{R}$ provides a statistically relevant indicator for the existence of a non–trivial topology on scales smaller than the catalog's limit.

---

[1] This labelling of the cells is inspired from the labelling of the principal axes in (ordinary) crystallography (see e.g. Phan (1990)).

Fig. 4. Plot of $\mathcal{R}(N)$ for the 3–torus T^3 with $B = 26$ copies.

Fig. 5. Plot of $\mathcal{R}(N)$ for the Weeks manifold with $B = 18$ copies.

4. Numerical simulations

In the previous section we have shown how $\mathcal{R}$ is a good indicator of the existence of a topological lensing. We now test our new method numerically and show how to implement it. For that purpose, assuming a locally hyperbolic space, we generate a toy catalog of cosmic sources as explained in Lehoucq et al. (1999) and we compute the CCP–index.

First, we need to determine the radial distance as a function of redshift (since the catalogs provide the angular coordinate and the redshift of the sources), which implies knowledge of the cosmological parameters. The local geometry is given by the Friedmann-Lemaître hyperbolic metric

$$ds^2 = -dt^2 + a^2(t)\left(d\chi^2 + \sinh^2 \chi d\Omega^2\right) \tag{12}$$

where a is the scale factor, t the cosmic time and $d\Omega^2 \equiv d\theta^2 + \sin^2 \theta d\varphi^2$ the infinitesimal solid angle.

We compute the relation between the radial coordinate distance (χ) and the object's redshift z. We start from the Einstein equations for the metric (12)

$$H^2 = \kappa \frac{\rho_m}{3} - \frac{K}{a^2} + \frac{\Lambda}{3}, \tag{13}$$

ρ_m being the matter density, Λ the cosmological constant and $\kappa \equiv 8\pi G/c^4$. H is the Hubble constant defined by $H \equiv \dot{a}/a$ with $\dot{X} \equiv \partial_t X$. We choose the units such that the curvature index is $K = -1$. Introducing $\Omega_\Lambda \equiv \Lambda/3H^2, \Omega_m \equiv \kappa\rho_m/3H^2$ and the redshift z defined by $1+z \equiv a_0/a$, (13) can be rewritten as (see e.g. Peebles (1993))

$$\frac{H^2}{H_0^2} = \Omega_{m0}(1+z)^3 + \Omega_{\Lambda 0} + (1 - \Omega_{m0} - \Omega_{\Lambda 0})(1+z)^2. \tag{14}$$

We have used Eq. (13) evaluated today (i.e. at $t = t_0$) and we have assumed that we were in a matter dominated universe, so that $\rho_m \propto a^{-3}$ (this hypothesis is very good since we restrict ourselves to small redshifts).

The radius of the observable region at a redshift z is given by integration of the radial null geodesic equation $d\chi = dt/a$

Fig. 6a and b. When the cosmological parameters are well estimated, the redshift–distance relationship enables to reconstruct the isometries **a**. However, when the estimation is wrong, all the determination of the radial distances are biased and there is no more correlated pairs in the coordinate space **b**. The observer is represented by the square sitting at the centre.

and reads

$$\chi(z) \equiv \int_{a_0}^{a} \frac{da}{a\dot{a}}$$

$$= \int_{\frac{1}{1+z}}^{1} \frac{\sqrt{1 - \Omega_{m0} - \Omega_{\Lambda 0}}dx}{x\sqrt{\Omega_{\Lambda 0}x^2 + (1 - \Omega_{m0} - \Omega_{\Lambda 0}) + \frac{\Omega_{m0}}{x}}}. \tag{15}$$

Eq. (15) is integrated numerically and the result can be compared, when $\Omega_\Lambda = 0$, to the analytic expression (see e.g. Gradstheyn & Ryzhik (1980))

$$\chi(z) = \left[\arg\cosh\left(1 + \frac{2(1 - \Omega_{m0})}{\Omega_{m0}}x\right)\right]_{\frac{1}{1+z}}^{1}. \tag{16}$$

The determination of the radial distance requires the knowledge of the cosmological parameters Ω_0 and Λ and can be obtained analytically only when $\Lambda = 0$. Thus, if the universe is multi-connected on sub–horizon scale, the plot of $\mathcal{R}$ in terms of Ω_0 and Ω_Λ should exhibit a spike only when the cosmological parameters have the right value (as shown in Fig. 7). If the cosmological parameters are not exactly known, the distance (15) will be ill-determined and the topological signature will be destroyed (see Fig. 6).

This has two consequences:

1. One should span the parameters space $(\Omega_0, \Omega_\Lambda)$ in order to detect the topological signal, plotting $\mathcal{R}(\Omega_0, \Omega_\Lambda)$.
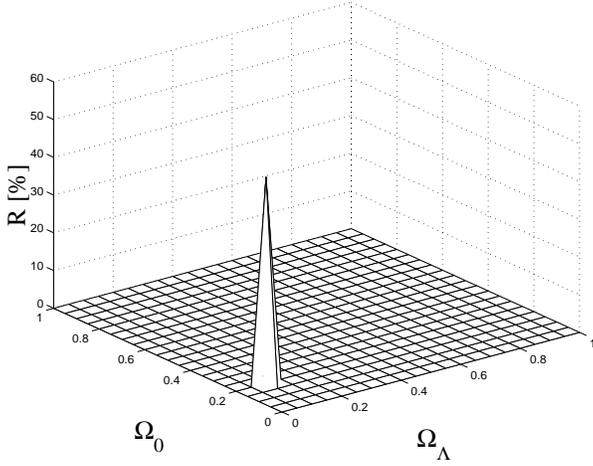
Fig. 7. Weeks $A = 30$, $\Omega_0 = 0.2$, $\Omega_\Lambda = 0.1$, $z = 3$ (quasars). We check that the topological signal stands out only at the right values of the cosmological parameters selected for the simulation.
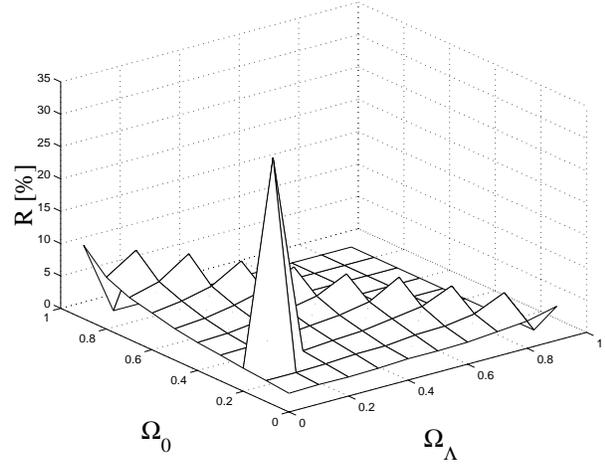

Fig. 8. Computation of the CCP–index on a simulated catalog of depth $z = 3$ in a hyperbolic universe model with the Weeks topology, $\Omega_0 = 0.3$, $\Omega_\Lambda = 0.1$, using a bin width $\epsilon = 10^{-6}$.

2. If there is any topological signal, the position of the spike gives the values of the cosmological parameters on the scale of the catalog's limit (see Fig. 7).

As a concrete example we proceed as follows. We first generate a simulated catalog by choosing the number of objects in the fundamental domain ($A = 30$), the topology (Weeks manifold) and the cosmological parameters (e.g. $\Omega_0 = 0.2$, $\Omega_\Lambda = 0.1$), and we then use a second code to apply the test, drawing $\mathcal{R}$ in terms of the two cosmological parameters. The result is shown in plot 7. We see that the method works pretty well in the sense that there is a spike signalling the presence of a topology and determining the cosmological parameters. But we also can check that a slight deviation in the choice of the cosmological parameters makes the spike to disappear. This effect will be discussed in the next section.

Now, if applied with the required accuracy for the cosmological parameters, the absence of signature will give the lower bound on the injectivity radius of the universe (in physical units)

$$\frac{r_{\mathrm{inj}}}{3000\,h^{-1}\,\mathrm{Mpc}}$$
$$\geq \int_{\frac{1}{1+z_{\max}}}^{1} \frac{\mathrm{d}\ln x}{\sqrt{\Omega_\Lambda x^2 + (1 - \Omega_0 - \Omega_\Lambda) + \frac{\Omega_0}{x}}}. \tag{17}$$

5. Working with real data

When one wants to apply the CCP–method to real data, one faces a number of problems. First, we cannot use a zero width bin, one of the reasons being that the sources are not exactly comoving. Let us first estimate the precision needed for the cosmological parameters when working with a bin of width ϵ as defined in Eq. (6). For that purpose, we just assume $\Omega_\Lambda = 0$ and estimate the precision on Ω_0 from (16),

$$\left| \frac{\delta\Omega_0}{\Omega_0} \right| = \sqrt{1 - \Omega_0}\, \frac{\sqrt{\Omega_0 z + 1}}{\sqrt{\Omega_0 z + 1} - 1}\,\epsilon \equiv F(\Omega_0, z)\epsilon. \tag{18}$$

Assuming $\Omega_0 \in [0.2, 1[$ and $z \in]0, z_{\max}]$, it is easy to see that at Ω_0 fixed, $F(\Omega_0, z)$ is a decreasing function of z and that $F(\Omega_0, z) \to \infty$ when $z \to 0$. Since $F(\Omega_0, z_{\max} = 3) \sim 1$, we deduce that

$$\left| \frac{\delta\Omega_0}{\Omega_0} \right| \simeq \epsilon. \tag{19}$$

Indeed, using a catalog with a smaller depth $z_{\max}$ will allow us to use a smaller resolution for the cosmological parameters. One has thus to find a compromise between depth and resolution. A deeper catalog tests larger topological scales, but requires a better accuracy of the cosmological parameters and thus a longer computer time. In Fig. 8, we give an example with a bin width $\epsilon = 10^{-6}$. The binning produces a "background noise" which was absent in Fig. 7.

As real data we now consider a quasar catalog[2] (Veron-Cetty & Veron 1998) containing 11,301 objects up to a redshift of $z_{\max} = 4.897$ (but only 20% of the quasars have a redshift greater than 3). On Figs. 9 we have depicted its projection on the celestial sphere and the redshift distribution of objects. In Uzan et al. (1999) the pair separation histogram method, valid only in Euclidean spaces, was applied to the same catalog and no topological signal was found; this raised the lower bound on the characteristic size of Euclidean space to $L \geq 3000\,h^{-1}\mathrm{Mpc}$. This limit, corresponding to $L_0/R_H \geq 0.5$, is of the same order as the bound $L_0/R_H \geq 0.8$ obtained from the CMB (Stevens et al. 1993).

We now apply the CCP–method in the Weeks hyperbolic space model assuming $\Omega_\Lambda = 0$ and Ω_0 spanning $[0.2, 0.9]$. No topological signal is found either. Does it mean that there is no topological lens effect on scales smaller than $z_{\max} \simeq 3$? Not necessarily, because we could only apply the test with precisions $\epsilon = 10^{-7}, 10^{-6}, 10^{-5}$, and were unable to span the cosmological parameter space with the required accuracy given by (19).

---

[2] although quasars are not as good standard candels as X–ray galaxy clusters, see Luminet & Roukema (1999) for a detailed discussion.
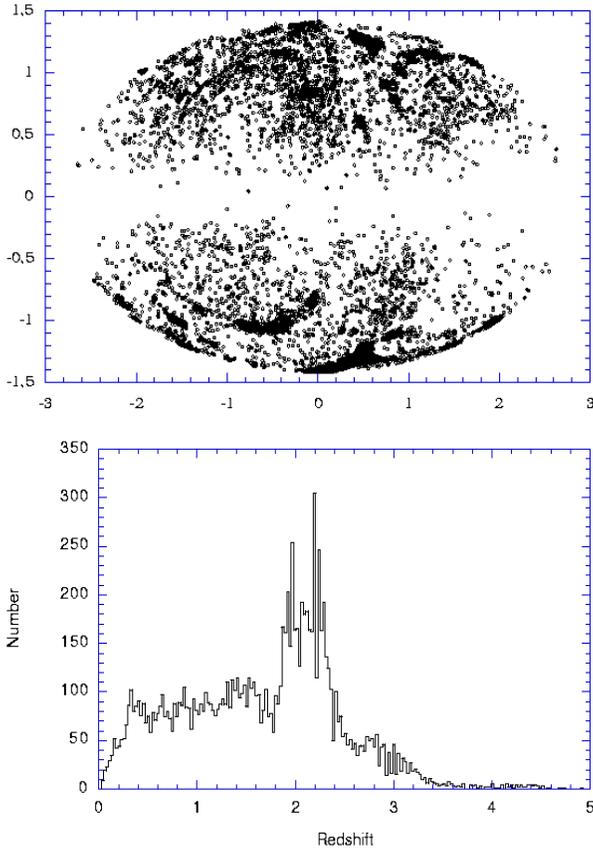
Fig. 9. The quasars catalog: (up) the distribution of objects on the celestial sphere in Hammer-Aitoff equal area projection; (down) the redshift distribution.

The computer time is one of the main limitations of our technique. It depends on the number of sources in the catalog. Typically, for the quasar catalog, we had to order about 64 millions pair increments (4) and the run took about 3 minutes (on a SUN Ultra Enterprise 3000 with a 1 Gbytes RAM) for each couple of cosmological parameters (Ω_0, Ω_Λ). Spanning the full set of reliable values ($[0, 1] \times [0, 1]$ with their sum smaller than 1) with a given resolution $\delta\Omega/\Omega$ requires a total running time proportional to $(\delta\Omega/\Omega)^{-2}$. Indeed, future observations will hopefully tighten the range of the cosmological parameters real values; as a consequence, we will have to span a smaller set of the cosmological parameters and our simulations will escape the present computer time limitations.

Now, a second limitation comes from the peculiar velocities of the sources. Assuming a typical peculiar velocity $v_p \simeq 500\,\mathrm{km\,s^{-1}}$ (see e.g. Dekel (1994)) the comoving position of a given object with respect to the observer is shifted by the quantity $\alpha(z)$ such that:

$$\alpha(z) \simeq v_p \frac{\tau(z)}{a_0}, \tag{20}$$

where $\tau(z)$ is the look-back time. It can be computed following the same lines as for the computation of (15), which leads to

$$\frac{\tau(z)}{a_0} = \int_{\frac{1}{1+z}}^1 \frac{\sqrt{1 - \Omega_{m0} - \Omega_{\Lambda 0}}\,\mathrm{d}x}{\sqrt{\Omega_{\Lambda 0}x^2 + (1 - \Omega_{m0} - \Omega_{\Lambda 0}) + \frac{\Omega_{m0}}{x}}}. \tag{21}$$

It follows that, since $x \leq 1$ in the integrals (15) and (21),

$$\frac{\tau(z)}{a_0} < \frac{\chi(z)}{c}, \tag{22}$$

so that

$$\alpha(z) < \frac{v_p}{c}\chi(z) \simeq 10^{-3}.\chi(z), \tag{23}$$

where $\chi(z)$ is the radial distance of the object given by (16). α is the uncertainty in the comoving position of a source *with respect to the observer*. We show below that the corresponding uncertainty induced in the pair separation distances is much smaller.

– For xy–pairs (see Fig. 10-a), the space position x' is related to its strictly comoving position $g(x)$ by

$$x' \simeq g(x) + \frac{\boldsymbol{v}_p(x)}{c}\mathrm{dist}[x, g(x)], \tag{24}$$

from which we deduce that

$$\mathrm{dist}[x', y'] \simeq \mathrm{dist}[g(x), g(y)] + (\boldsymbol{xy}.\boldsymbol{\nabla})\frac{v_p(x)}{c}.\frac{\boldsymbol{xy}}{\mathrm{dist}[x, y]}$$
$$+ \frac{\boldsymbol{v}_p(x)}{c}\frac{(\mathrm{dist}[x, g(x)] - \mathrm{dist}[y, g(y)])}{\mathrm{dist}[x, y]}.\boldsymbol{xy}. \tag{25}$$

Since $\mathrm{dist}[g(x), g(y)] = \mathrm{dist}[x, y]$ the uncertainties come from two factors

1. the velocity gradient; however, assuming large scale velocity flows, two neighbouring images have similar peculiar velocities and the gradient is very small.
2. a term proportional to the difference of separation distances, which vanishes if g is a Clifford translation. Otherwise (as seen in Fig. 11 of Lehoucq et al. (1999)), for neighbouring points $\mathrm{dist}[x, g(x)] - \mathrm{dist}[y, g(y)] \ll r_+$, where r_+ is the largest characteristic size of the manifold [i.e. the radius of the smallest geodesic ball containing the fundamental domain, see e.g. Fig. 10 in Luminet & Roukema (1999)].

Indeed, we will lose some of the signal from pairs between far apart objects.

– For $xg(x)$–pairs (see Fig. 10-b) the position of $g_i(x)$ is shifted by $\boldsymbol{v}_p(x)\mathrm{dist}[x, g_i(x)]/c$ so that

$$\mathrm{dist}[x_3', x_{13}'] \simeq \mathrm{dist}[g_3(x), g_3 \circ g_1(x)] + \frac{\boldsymbol{v}_p(x)}{c}.\boldsymbol{xg_1(x)}$$
$$\frac{(\mathrm{dist}[x, g_1 \circ g_3(x)] - \mathrm{dist}[x, g_1(x)])}{\mathrm{dist}[g_3(x), g_1 \circ g_3(x)]}. \tag{26}$$

Since $\mathrm{dist}[g_3(x), g_3 \circ g_1(x)] = \mathrm{dist}[x, g_1(x)]$, it is easy to see that

$$\mathrm{dist}[x_3', x_{13}'] - \mathrm{dist}[x_2', x_{12}'] \simeq \frac{\boldsymbol{v}_p(x)}{c}.\boldsymbol{xg_1(x)} \times$$
$$\frac{(\mathrm{dist}[x, g_2 \circ g_3(x)] - \mathrm{dist}[x, g_1 \circ g_3(x)])}{\mathrm{dist}[x, g_1(x)]}. \tag{27}$$
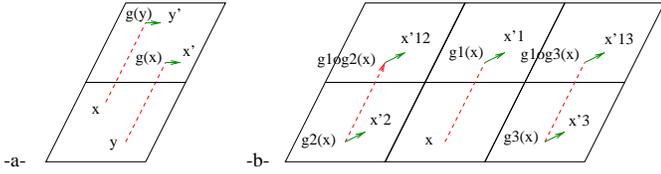
Fig. 10a and b. Due to peculiar velocities, two topological images are shifted from their strictly comoving position. We represent here the relation between the mathematical images $[g_i(x)]$ and the topological images $[x'_i]$ **a** for xy-pairs and **b** for $xg(x)$-pairs.

This strictly vanishes if, for instance, $g_2 = g_1^{-1}$. Otherwise, $\text{dist}[x, g_2 \circ g_3(x)] - \text{dist}[x, g_1 \circ g_3(x)]$ is much smaller than r_+. This can be understood from the fact that the look-back times of $g_2 \circ g_3(x)$ and $g_1 \circ g_3(x)$ are of the same order and anyway, their difference is much smaller than the expected time for a photon to wrap around the universe.

To our knowledge, such a discussion about the uncertainty introduced by proper velocities on the positions of topological images has never been correctly addressed. Although the uncertainty induced by proper velocities is low, it will cause the CCP–index to be smaller than its theoretical value, since some correlated pairs constructed from far apart images will be lost. However, the uncertainty could further be reduced if, for instance, we were able to obtain a 6–D catalog including the peculiar velocities, in order to correct the position from the shift given by (24), assuming that this velocity field has a weak time dependence. One also has to take into account the uncertainty in distance determination and spectroscopic errors (see (Roukema 1996) for a discussion of these effects).

6. Conclusions

In this article we have introduced a new method for detecting the topology of the spatial sections of the universe using 3D–catalogs of discrete sources. The main motivation for looking for such a method was the failure of the standard cosmic crystallography for detecting the topology of locally hyperbolic spaces.

Our method is based on the construction of a *CCP–index* as detailed in Sect. 3. The main difference with the cosmic crystallography is the collecting process of all correlated pairs in the catalog, which enhances the signal associated to the existence of a non trivial topology. We then showed the statistical relevance of this new method both on analytic computations and on numerical simulations.

Indeed, all the simulations were based on an idealised method applied to idealised catalogs. We then took into account more realistic situations, discussing the effect of the finite width of the bins, of the peculiar velocities of the objects and of their distance uncertainties (Sect. 5).

To finish, we applied our method to a quasar catalog and found no topological signature. As explained in Sect. 5, this does not prove that the topological scale of the universe is larger than the catalog's size because we were limited by computer time in spanning the full parameter space with the required accuracy.

To achieve this task, we would have to test around 10^6 couples of cosmological parameters, giving a total computation time on our SUN workstation greater than five years. A reasonable computation time can be obtained by increasing the calculation speed by two orders of magnitude at least. Thus, we are now trying to implement our method on a Cray T3E parallel computer with 288 DEC Alpha processors in order to gain a factor of at least 100 in computation time. It is worth noting that total scanning of the parameter space can be done by few hundreds computers since couples of cosmological parameters can be tested independently.

Indeed, we have to wait for tighter constraints on the cosmological parameters coming from various sides of observational cosmology (see e.g. the proceedings of the XXXIII$^{\text{rd}}$ Rencontres de Moriond (1998) for a review) in order to reduce the parameter space.

Now, it is clear that our method cannot help us determine the exact topology of the spatial sections of the universe. It will only provide a signature of the compactness of these spatial sections on scales smaller than the catalog depth. Indeed, once this information is known, one can think of developing a shape recognition code (for triplets, quadruplets, etc.) that will enable us to reconstruct the elements of the holonomy group [note that the group structure will allow us to reject false identifications and to infer the existence of missing objects in the catalog].

This approach can be thought of as the 3–D analog of the 2–D circles method using the cosmic microwave background data (Cornish et al. 1998a; Cornish et al. 1998b; Cornish et al. 1998c). The same as the COBE data does not have the required resolution to exhibit pairs of matched circles if the universe is small, and the technique also has to wait for future satellite missions such as MAP and Planck, the CCP–method is presently limited to 3–D catalogs with low redshifts. Until now we are limited to quasars ($z_{\text{max}} \simeq 3$). A recent survey (Chen et al. 1998) in the Hubble Deep Field south NICMOS field found 17 galaxies with redshifts between 5 and 10 and 5 galaxies with redshifts above 10, among a total of 323 galaxies. Such deep surveys can enable us hope that we may apply our method to deeper catalogs in the future. Also, just as the circle method will suffer from the degradation in the circle match caused by detector noise (see e.g. Fig. 7 of Cornish et al. (1998c)), our CCP–method suffers from degradation caused by velocity and distance uncertainties.

To finish, let us extrapolate a little. If the spatial sections of our universe have any (observationally relevant) topological property, the graph of $\mathcal{R}$ in terms of the two parameters $(\Omega_0, \Omega_\Lambda)$ should exhibit a resonance at the right value of these parameters (otherwise, the distance determination being wrong, no signature could be detected). Besides the detection of a non trivial topology, the CCP–method can help us determine the cosmological parameters on the scale of the catalog limit and will, in that case, be an interesting tool to use together with the other methods (theoretical and observational) designed to determine these parameters. Note that the CCP–method for determining the cosmological parameters is purely geometric, contrary to the ones using, e.g., the cosmic microwave background anisotropies

which assume a given scenario of structure formation. Thus, in the case of multi-connected universe, it will help to improve the estimation of these parameters from the CMB. Indeed this is, at the time being, only prospective.

In conclusion, our new crystallographic method is well backed up mathematically but suffers from practical implementation difficulties. It is, however, important to realise that a 3D–catalog of cosmic sources contains more information than previously suspected, and that the joint study of topology and cosmology can lead to a better determination of the curvature parameters.

References

Bond J. R., Pogosyan D., Souradeep T., 1998, Class. Quant. Grav. 15, 2671

Chen H.-W., Fernandez-Soto A., Lanzetta K. M., Pascarelle S. M., Puetter R. C., Yahata N., Yahil A., 1998, `astro-ph/9812339`

Cornish N. J., Spergel D. N., Starkman G. D., 1998a, Phys. Rev. D 57, 5982

Cornish N. J., Spergel D. N., Starkman G. D., 1998b, Proc. Nat. Acad. Sci. 95, 82

Cornish N. J., Spergel D. N., Starkman G. D., 1998c, Class. Quant. Grav. 15, 2657

de Oliveira Costa A., Smoot G. F., Starobinsky A. A., 1996, ApJ 468, 457

Dekel A., 1994, ARA&A 32, 371

Ellis G. F. R., 1971, Gen. Rel. Grav. 2, 7

Fagundes H. V., Gaussmann E., 1997, Phys. Lett. A 238, 235

Fagundes H. V., Gaussmann E., 1998, `astro-ph/9811368`

Fagundes H. V., Wichoski W. F., 1987, ApJ 322, L5

Gibbons G. W., Starkman G. D. (eds.), 1998, Cosmology and topology, Vol. 15, Class. Quant. Grav.

Gomero G. I., Teixeira A. F. F., Rebouças M. J., Bernui A., 1998, `gr-qc/9811038`

Gott J. R., 1980, MNRAS 193, 153

Gradstheyn I. S., Ryzhik I. M., 1980, Table of integrals series and products, Academic N.Y.

Hawking S., Ellis G. F. R., 1973, Large scale structure of spacetime, Cambridge university Press

Inoue K. T., 1998, `astro-ph/9810034`

Lachièze-Rey M., Luminet J.-P., 1995, Phys. Rep. 254, 135

Lehoucq R., Lachièze-Rey M., Luminet J.-P., 1996, A&A 313, 339

Lehoucq R., Luminet J.-P., Uzan J.-P., 1999, A&A 344, 735, `astro-ph/9810107`

Levin J.J. Barrow J.D., Bunn E., Silk J., 1997, Phys. Rev. Lett. 79, 974

Levin J.J. Scannapieco E., Silk J., 1998, Phys. Rev. D 58, 103516

Luminet J.-P., Roukema B. F., 1999, in Observational and Theoretical Cosmology, Cargese 98 Summer school, Kluwer, `astro-ph/9901364`

Peebles P. J. E., 1993, Principles of Physical Cosmology, Princeton university Press

Phan K. D., 1990, Cours de cristallographie, École Nationale Supérieures des Mines de Paris, Paris

Roukema B. F., 1996, MNRAS 283, 1147

Roukema B. F., Edge A. C., 1997, MNRAS 292, 105

Sokolov D. D., 1971, Sov. Phys. Dokl. 15, 112

Stevens D., Scott D., Silk J., 1993, Phys. Rev. Lett. 71, 20

Thurston W. P., 1997, Three Dimensional Geometry and Topology, Princeton University Press

Trân Thanh Vân J. (ed.), 1998, Fundamental parameters in cosmology, XXXIIIrd Rencontres de Moriond, Éditions frontières

Uzan J.-P., 1998a, Phys. Rev. D 58, 087301

Uzan J.-P., 1998b, Class. Quant. Grav. 15, 2711

Uzan J.-P., Lehoucq R., Luminet J.-P., 1999, in P. Peter (ed.), Relativistic astrophysics, XIXth Texas symposium, Paris, 14-18 december 1998

Veron-Cetty M. P., Veron P., 1998, Catalog VII/207, Quasars and Active Galactic Nuclei, 8th edition, `http://cdsweb.u-strasbg.fr/viz-bin/VizieR?-source=VII/207/`

Weeks J., 1985, Ph.D. thesis, Princeton University

Wolf J. A., 1984, Spaces of constant curvature, Publish or Perish Inc., Wilmington (USA), fith edition